Properties of inverted polymer solar cells based on novel small molecular electrolytes as the cathode buffer layer

Youn Hwan Kim [a], Nadhila Sylvianti [a], Mutia Anissa Marsya [a], Doo Kyung Moon [b], Joo Hyun Kim [a, *]

[a] Department of Polymer Engineering, Pukyong National University, Busan, 48547, South Korea
[b] Department of Materials Chemistry and Engineering, Konkuk Univerisity, Seoul, 05029, South Korea

ARTICLE INFO

ABSTRACT

Novel small-molecule electrolytes were designed and synthesized for use in the cathode interlayer in bulk-heterojunction polymer solar cells (PSCs). The synthesized materials consist of polar quaternary ammonium bromide with the addition of multiple hydroxyl groups, which are N,N,N,N,N,N-hexakis(2-hydroxyethyl)butane-1,4-diaminium bromide (**C4**) and N,N,N,N,N,N-hexakis(2-hydroxyethyl)hexane-1,6-diaminium bromide (**C6**). The materials generate a favorable interface dipole through the quaternary ammonium bromide. In addition, the multiple polar hydroxyl groups increased the interface dipole magnitude. The power conversion efficiency of the devices with the interlayer was up to 9.20% with a J_{sc} of 17.22 mA/cm^2, a V_{oc} of 0.75 V, and an FF of 71.3%. The PCE of devices with an interlayer show better long-term stability than a device without an interlayer. Our strategy shows that it is possible to enhance the efficiency of PSCs by simple approaches without complicated syntheses.

© 2016 Elsevier B.V. All rights reserved.

1. Introduction

Recently, bulk-heterojunction (BHJ) polymer solar cells (PSCs) have attracted attention due to their high potential for application as clean energy sources, as they are lightweight, flexible, and capable of large-area fabrication [1–4]. The power conversion efficiencies (PCEs) of PSCs have improved rapidly. PCEs of over 10% have been reported, due to tremendous efforts made in areas such as the synthesis of new conjugated polymers/oligomers [5,6] and interface engineering [7]. Charge transport and collection properties at both electrode interfaces are crucial factors for improving the efficiency of PSCs. Significant work has been undertaken to improve interfacial properties, such as alcohol/water soluble conjugated polymer electrolytes (CPEs) [8–17], non-conjugated polymers [18–23], alcohol/water soluble conjugated [24–27] or non-conjugated small molecules (SMs) [28–30], and polar solvent treatment [31–35]. These materials enable the fabrication of a multilayer device without destroying a pre-coated organic semiconducting layer by orthogonal solubility in the processing solvents. PSCs with a thin film of these materials as an interlayer (IL) at

the cathode interfaces show dramatically improved performance, relative to the devices manufactured without these materials as an interfacial layer. It has been reported that the ionic functionalities, at the end of side chains on the conjugated polymer backbone, induce the formation of favorable interface dipole, which leads to a decrease in the work function of the cathode. Non-conjugated polymers or SMs [28–35] can also reduce the work function of the cathode due to the formation of an interface dipole. In comparison with polymeric materials, SMs have advantages such as ease of synthesis and purification. In addition, SMs do not have batch-to-batch variation, or broad molecular weight distribution.

In this research, we designed and synthesized non-conjugated SM organic electrolytes, which consist of polar quaternary ammonium bromide with the addition of multiple hydroxyl groups. The structure of SM electrolytes used in this research, N,N,N,N,N,N-hexakis(2-hydroxyethyl)butane-1,4-diaminium bromide (**C4**) and N,N,N,N,N,N-hexakis(2-hydroxyethyl)hexane-1,6-diaminium bromide (**C6**), are shown in Fig. 1. In order to observe the effect of hydrophobicity of the on the interfacial properties, we introduced different lengths of alkyl chains in between **C4** and **C6**. The thin layer of SMs in this research generated a favorable interface dipole with the quaternary ammonium bromide. In addition, the magnitude of the interface dipole was increased by the multiple polar hydroxyl groups at the end of **C4** and **C6**. Inverted PSCs (iPSCs), with
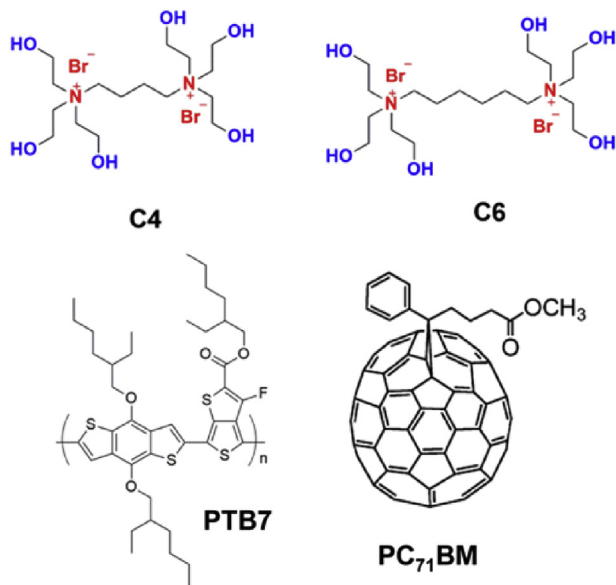

Fig. 1. Chemical structure of **C4**, **C6**, and materials in this research.

a structure of ITO/ZnO/**C4** or **C6**/PTB7:PC$_{71}$BM(1:1.5)MoO$_3$/Ag, were fabricated to investigate the effect of the IL on photovoltaic properties. A thin layer of **C4** and **C6** as the IL between the ZnO layer and the active layer in the iPSC dramatically improved the short circuit current density (J$_{sc}$), and the fill factor (FF), resulting in a PCE improvement from 7.41% to 9.20%, which is a 24.2% relative enhancement. The open circuit voltage (V$_{oc}$) data of the device with the ILs are almost same as the data of the reference device. Enhancements of the PCE of the devices were primarily due to the improvement of the J$_{sc}$. The ILs facilitate charge extraction from the

active layer to the cathode due to their favorable interface dipole, which reduces the energy barrier at the cathode interface, i.e., transition from a Schottky to an Ohmic contact.

2. Results and discussion

To investigate the effect of ILs on photovoltaic properties, iPSCs with the structure ITO/ZnO or IL/PTB7:PC$_{71}$BM/MoO$_3$/Ag (as shown in Fig. 2 (a)) were fabricated. The current density vs. voltage curves of the iPSCs under AM 1.5G simulated illumination with an intensity of 100 mW/cm^2 and in the dark are shown in Fig. 2 **(c)**. The device performances are summarized in Table 1. The V$_{oc}$ and FF of the device based on ITO/**C4** and ITO/**C6** were smaller than the device based on ITO/ZnO while the J$_{sc}$ of the devices based on ITO/**C4** and ITO/**C6** increased slightly from 14.65 mA/cm^2 to 14.95 and 15.33 mA/cm^2, respectively. Thus, the PCE of the devices based on ITO/**C4** and ITO/**C6** are 6.03 and 6.65%, respectively, which are lower than the device based on ITO/ZnO (7.35%).

Kelvin probe microscopy (KPM) measurements were performed to investigate the effective work function of IL coated ITO and the ITO/ZnO surface and to prove the formation of an interface dipole at the surface of the substrate. The work function of **C4** and **C6** coated ITO with IL decreased from 5.0 eV (the work function of ITO) to 4.76 and 4.86 eV, respectively. These values are greater than that of ITO/ZnO (4.4 eV). The energy barrier height between the work function of IL coated ITO and the LUMO level of PC$_{71}$BM is larger than that of ITO/ZnO (as illustrated in Fig. 2 (b)). Thus, the performance of devices based in IL coated ITO are lower than those of devices based on ITO/ZnO. The work function data from the KPM measurements support the findings that the performance of a device with IL is lower than that of a device based on ITO/ZnO. The series resistance (R$_s$) values of the devices based on IL coated ITO are lower than that of devices based on ITO/ZnO. The leakage current (inset of Fig. 2 **(c)**)
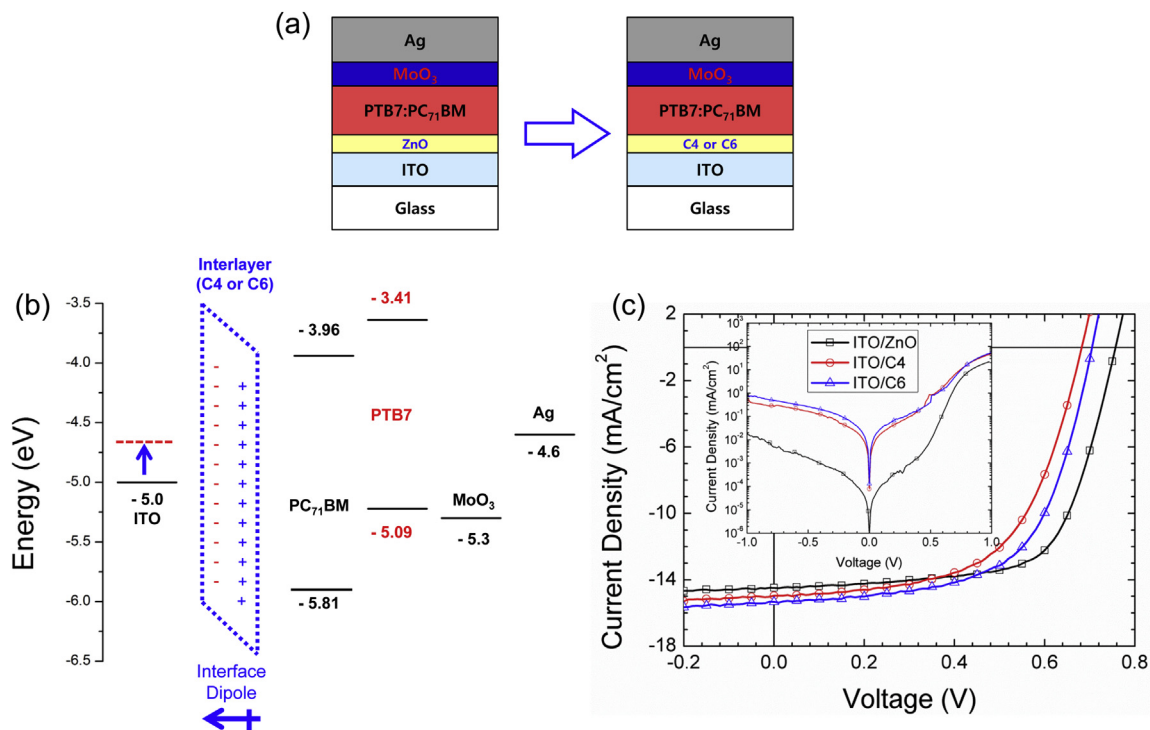

Fig. 2. Schematic illustration of (a) the device structures based on ITO/ZnO and ITO/**C4** or **C6**, (b) the energy level diagram of materials in this research, and (c) current density–voltage curves of iPSCs under AM 1.5G simulated illumination with an intensity of 100 mW/cm^2 (inset: in the dark condition; square: with ITO/ZnO; circle: with ITO/**C4**; triangle: with ITO/**C6**).

Table 1

Summary of photovoltaic parameters of iPSCs based on ZnO, ITO/**C4**, and ITO/**C6** with the best PCE value. The averages (8 devices are averaged) of photovoltaic parameters for each device are given in parentheses.

Buffer layer	J_{sc} (mA/cm^2)	V_{oc} (V)	FF (%)	PCE (%)	R_s^a (Ω cm^2)	R_{sh}^b (kΩ cm^2)
ZnO	14.48 (14.15)	0.76 (0.76)	66.8 (67.5)	7.35 (7.26)	10.4	0.38
ITO/**C4**	14.95 (14.98)	0.68 (0.68)	59.3 (58.6)	6.03 (5.94)	4.1	0.035
ITO/**C6**	15.33 (15.10)	0.71 (0.71)	61.1 (62.0)	6.65 (6.61)	3.5	0.045

[a), b)] series and shunt resistance, respectively (estimated from the device with the best PCE).

evices with IL coated ITO are significantly higher than that of the device based on ITO/ZnO. This is due to the shunt resistance (R_{sh}) of devices based on IL coated ITO being significantly lower than that of the device based on ITO/ZnO. The smaller R_{sh} value and large leakage current are also possible reasons that devices based in IL coated ITO exhibit lower PCE than that of the device based on ITO/ZnO.

To enhance the performance of devices without sacrificing V_{oc} and FF, iPSCs were fabricated, based on IL coated ITO/ZnO. Current density vs. voltage relationships of the iPSCs with the structure ITO/ZnO/with or without IL/PTB7:PC$_{71}$BM/MoO$_3$/Ag (as shown in Fig. 3 (a)) under the AM 1.5G simulated illumination with an intensity of 100 mW/cm^2 and in the dark are shown in Fig. 3 (c). Device performances are summarized in Table 2. For conventional PSCs, it has been reported that polar solvent treatment at the cathode interface showed a positive effect on the performance of the devices [31–35]. To remove the possible synergy effect of the interlayer processing solvent (methanol), the ZnO layer of reference devices was treated with methanol. The J_{sc} of the methanol treated device slightly increased from 14.48 mA/cm^2 to 14.65 mA/cm^2, while the V_{oc} and J_{sc} were almost identical. This indicates that methanol does not significantly affect the performance of the iPSCs in this research;

however, methanol could reduce defects in the ZnO surface. The J_{sc} values of devices with **C4** and **C6** are 17.22 and 16.78 mA/cm^2, respectively, which are a significant improvement over the device without an interlayer (14.65 mA/cm^2). The FF of the devices based on **C4** and **C6** also increased from 66.6% to 71.3% and 72.4%, respectively. The device with **C4** and **C6** as the cathode IL shows the highest PCE values of 9.20 and 9.11%, respectively, indicating that the **C4** and **C6** layer induces a favorable interface dipole at the cathode interface in the devices. It should be noted that the highest increase in the PCE of devices with IL results from enhancement of the J_{sc}. The effective work function of **C4** and **C6** coated ZnO surface calculated from the KPM measurements are 3.98 and 3.99 eV, respectively, which are a decrease from the work function of methanol treated ZnO (4.4 eV). This is due to the formation of a favorable interface dipole by the thin layer of **C4** and **C6** on the ZnO surface. Note, the J_{sc} results strongly related to the work function data. Ohmic contact at the interfaces is required to obtain a high J_{sc}. However, a large Schottky barrier height interrupts charge collection at the cathode interface. J_{sc} improvement, in addition to the PCE change showing good correlation with the change in the work function, indicates a typical transition from a Schottky to an Ohmic contact. Interestingly, the V_{oc} of the devices with ILs is almost same
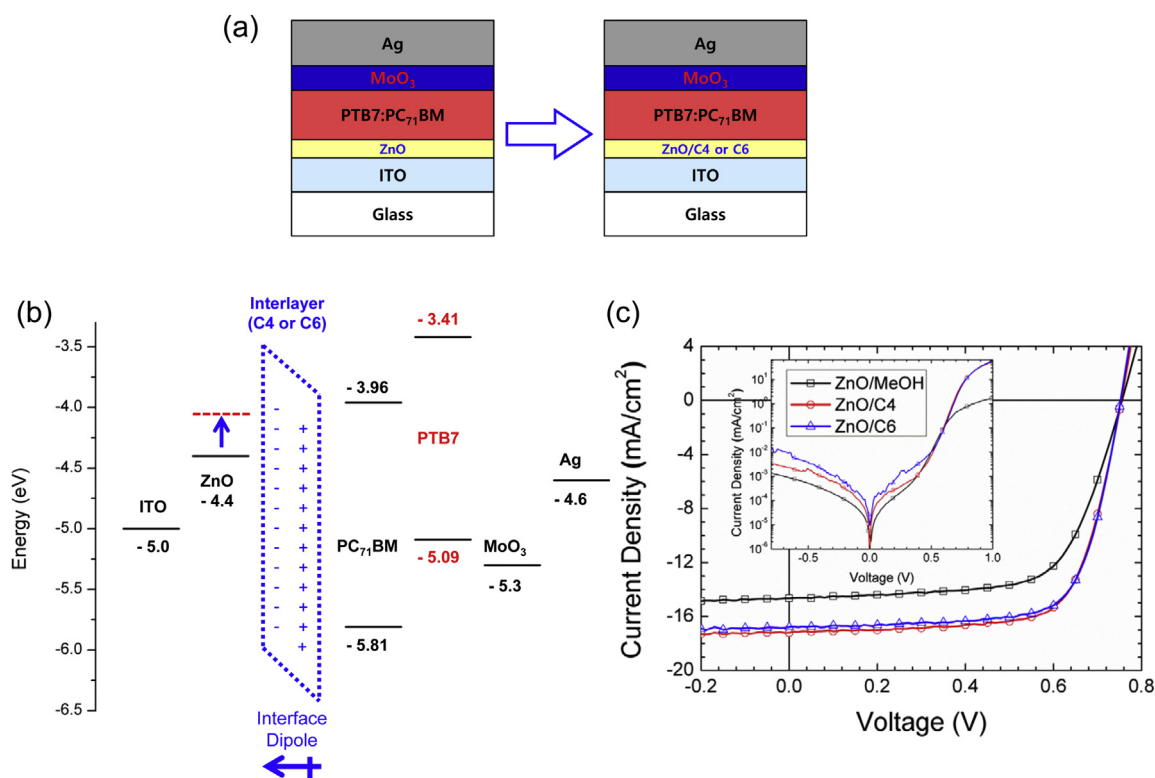
Fig. 3. Schematic illustration of (a) device structures based on ZnO and ZnO/**C4** or **C6**, (b) the energy level diagram of materials in this research, and (c) current–voltage curves of iPSCs under (a) AM 1.5G simulated illumination with an intensity of 100 mW/cm^2 (inset: in the dark condition; square: with ITO/ZnO/MeOH; circle: with ITO/ZnO/**C4**; triangle: with ITO/ZnO/**C6**).

Table 2
Summary of photovoltaic parameters of iPSCs based on ZnO/MeOH, ZnO/**C4**, and ZnO/**C6** with the best PCE value. The averages (8 devices are averaged) of photovoltaic parameters for each device are given in parentheses.

Buffer layer	J_{sc} (mA/cm^2)	V_{oc} (V)	FF (%)	PCE (%)	R_s^a (Ωcm^2)	R_{sh}^b (kΩcm^2)
ZnO/MeOH	14.65 (14.25)	0.76 (0.75)	66.6 (66.2)	7.41 (7.08)	5.91	0.37
ZnO/**C4**	17.22 (16.97)	0.75 (0.75)	71.3 (71.0)	9.20 (9.10)	3.8	0.30
ZnO/**C6**	16.78 (15.67)	0.75 (0.75)	72.4 (71.7)	9.11 (9.06)	3.4	0.21

[a), b)] Series and shunt resistance, respectively (estimated from the device with the best PCE).

as the reference device. Even though the interlayer modifies the surface potential of the ZnO layer, it hardly affects the V_{oc} of the devices. The R_{sh} data of devices with IL are lower than those of the device based on ITO/ZnO. This correlates with devices with IL showing a larger leakage current under the reverse bias (as shown in the inset of Fig. 3 (c)). Devices with IL are estimated to have smaller R_s and larger FF values, indicating the formation of an Ohmic contact at the cathode interface. Even though the device with ILs exhibit larger leakage current and smaller the R_{sh}, the devices with PVA exhibited better Jsc and FF than those of the devices without IL.

The effect of IL on electron transport properties was investigated by a space charge limited current (SCLC) study of electron-only devices with a structure of ITO/ZnO/IL/PC$_{71}$BM/Al. The energy

Fig. 4. Current density–voltage curves of electron-only devices with fitted line of electron-only devices.

Fig. 5. IPCE spectra of the devices based on ZnO/MeOH, ZnO/**C4**, and ZnO/**C6**.

barrier between the LUMO level of PC$_{71}$BM and the work function of ZnO (cathode) layer and the HOMO level of PC$_{71}$BM the Al electrode (anode) were 0.44 and 2.01 eV, respectively. Thus, the major carriers in the device will be electrons under forward bias. Above the built-in electric field (as shown in Fig. 4), the current density and V-V$_{bi}$ (voltage - built-in voltage) exhibit a quadratic relationship, which is characteristic of SCLC. This can be expressed by the Mott-Gurney law [36].

$$J = \frac{9}{8}\varepsilon_0\varepsilon_r\mu\frac{E^2}{L}$$

where J is the current density, μ is the charge mobility, E is the electric field, $\varepsilon_0\varepsilon_r$ is the permittivity of the active layer, and L is the thickness of the active layer. Using $\varepsilon_r = 3.9$, [37] the current density and voltage relationship of the device agrees well with the Mott-Gurney Law. The electron mobilities of the device with **C4** and **C6** are 3.62×10^{-7} and 2.77×10^{-7} m^{2}V^{-1}s^{-1}, respectively, which are comparable to the value of the device without IL (3.17×10^{-7} m^{2}V^{-1}s^{-1}). Interestingly, the **C4** and **C6** layer hardly affects the electron mobility of the devices.

Surface morphology and properties were investigated by AFM and water contact angle measurements. As shown in Fig. S4 (see supporting information), the surface roughness of **C4** and **C6** coated ZnO are 1.50 and 1.48 nm, respectively, which are almost identical to that of the ZnO surface (1.44 nm). According to the water contact angle data (as shown in Fig. S5), the thin layer of coated ZnO surface became more hydrophilic than the surface of ZnO due to the intrinsic properties of the **C4** and **C6** materials. However, it is very hard to correlate the relationship between the hydrophobicity of the materials and device performance. The incident photon-to-current efficiency (IPCE) (Fig. 5) curves of the devices show very good agreement with the change of the Jsc data of the devices under 1.0 sun illumination.

The devices were subsequently kept in a nitrogen filled glove box without passivation. The device without IL maintained 79% of its initial PCE after 125 days. In contrast, the PCE of the devices with **C4** and **C6** showed better stability, retaining 86% and 90% of their initial PCE values, respectively, after 125 days.

3. Conclusion

A series of new alcohol/water soluble small molecules have been successfully synthesized with a skeleton of both a quaternary ammonium salt and multiple hydroxyl groups. A thin layer of **C4** and **C6** improves the J$_{sc}$, mainly due to the formation of a favorable interface dipole, which reduces the electron collection barrier. As a result, the PCE of the device with **C4** as the cathode IL shows the best PCE of 9.20% with a J$_{sc}$ of 17.22 mA/cm^2, a V$_{oc}$ of 0.75 V, and a FF of 71.3%. This research provides a very simple alternative strategy relative to device design using complicated synthesis.
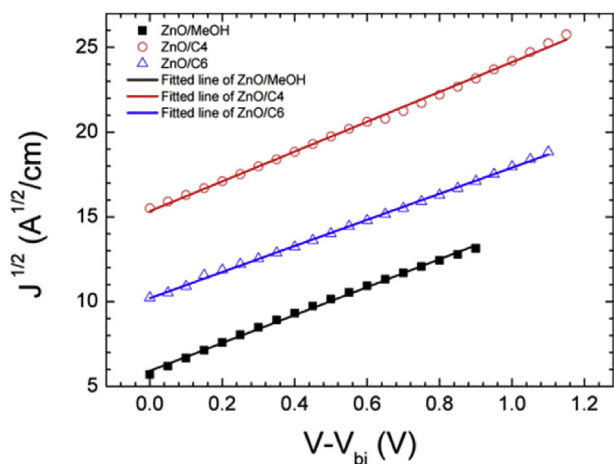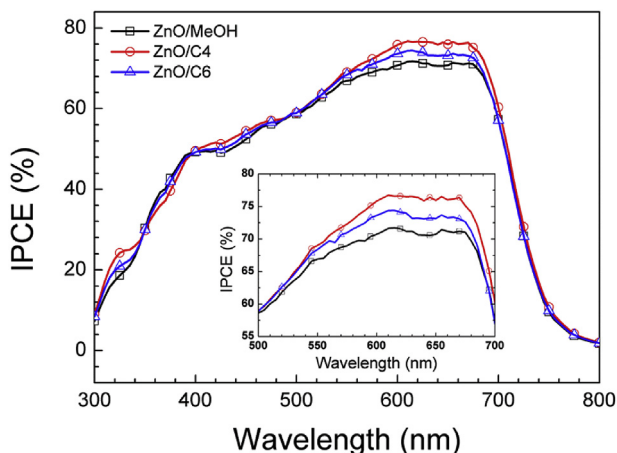
Appendix A. Supplementary data

Supplementary data related to this article can be found at http://dx.doi.org/10.1016/j.orgel.2016.09.035.

References

Experimental details including materials, material synthesis, measurements, and fabrication of device in addition to synthesis scheme, NMR spectra, AFM images, and water contact angle data are available in supplementary information

[1] G. Yu, J. Gao, J.C. Hummelen, F. Wudl, A.J. Heeger, Polymer photovoltaic cells: enhanced efficiencies via a network of internal donor-acceptor hetero-junctions, Science 270 (1995) 1789–1791.

[2] W.U. Huynh, J.J. Dittmer, A.P. Alivisatos, Hybrid nanorod-polymer solar cells, Science 295 (2002) 2425–2427.

[3] S. Gunes, H. Neugebauer, N.S. Sariciftci, Conjugated polymer-based organic solar cells, Chem. Rev. 107 (2007) 1324–1338.

[4] L. Lu, T. Zheng, Q. Wu, A.M. Schneider, D. Zhao, L. Yu, Recent advances in bulk heterojunction polymer solar cells, Chem. Rev. 115 (2015) 12666–12731.

[5] V. Vohra, K. Kawashima, T. Kakara, T. Koganezawa, I. Osaka, K. Takimiya, H. Murata, Efficient inverted polymer solar cells employing favourable molecular orientation, Nat. Photonics 9 (2015) 403–408.

[6] B. Kan, M. Li, Q. Zhang, F. Liu, X. Wan, Y. Wang, W. Ni, G. Long, X. Yang, H. Feng, Y. Zuo, M. Zhang, F. Huang, Y. Cao, T.P. Russell, Y. Chen, A series of simple oligomer-like small molecules based on oligothiophenes for solution-processed solar cells with high efficiency, J. Am. Chem. Soc. 137 (2015) 3886–3893.

[7] Y. Liang, Z. Xu, J.B. Xia, S.T. Tsai, Y. Wu, G. Li, C. Ray, L. Yu, For the bright future—bulk heterojunction polymer solar cells with power conversion efficiency of 7.4%, Adv. Mater. 22 (2010) E135–E138.

[8] Z. He, C. Zhong, S. Su, M. Xu, H. Wu, Y. Cao, Enhanced power-conversion efficiency in polymer solar cells using an inverted device structure. Enhanced power-conversion efficiency in polymer solar cells using an inverted device structure, Nat. Photonics 6 (2012) 591–595.

[9] H. Choi, J.S. Park, E. Jeong, G.W. Kim, B.R. Lee, S.O. Kim, M.H. Song, H.Y. Woo, J.Y. Kim, Combination of titanium oxide and a conjugated polyelectrolyte for high-performance inverted-type organic optoelectronic devices, Adv. Mater. 23 (2011) 2759–2763.

[10] S.H. Oh, S.I. Na, J. Jo, B. Lim, D. Vak, Y.D. Kim, Water-soluble polyfluorenes as an interfacial layer leading to cathode-independent high performance of organic solar cells, Adv. Funct. Mater. 20 (2010) 1977–1983.

[11] W. Ma, P.K. Iyer, X. Gong, B. Kiu, D. Moses, G.C. Bazan, A.J. Heeger, Water/Methanol-Soluble conjugated copolymer as an electron-transport layer in polymer light-emitting diodes, Adv. Mater. 17 (2005) 274–277.

[12] Y. Jin, G.C. Bazan, A.J. Heeger, J.Y. Kim, K. Lee, Improved electron injection in polymer light-emitting diodes using anionic conjugated polyelectrolyte, Appl. Phys. Lett. 93 (2008), 123304–1 -123304-3.

[13] X. Zhu, Y. Xie, X. Li, X. Qiao, L. Wang, G. Tu, Anionic conjugated poly-electrolyte—wetting properties with an emission layer and free ion migration when serving as a cathode interface layer in polymer light emitting diodes (PLEDs), J. Mater. Chem. 22 (2012) 15490–15494.

[14] J. Fang, B.H. Wallikewitz, F. Gao, G. Tu, C. Muller, G. Pace, R.H. Friend, W.T.S. Huck, Conjugated zwitterionic polyelectrolyte as the charge injection layer for high-performance polymer light-emitting diodes, J. Am. Chem. Soc. 133 (2011) 683–685.

[15] F. Huang, Y. Zhang, M.S. Liu, A.K.Y. Jen, Electron-rich alcohol-soluble neutral conjugated polymers as highly efficient electron-injecting materials for polymer light-emitting diodes, Adv. Funct. Mater. 19 (2009) 2457–2466.

[16] H. Wu, F. Huang, Y. Mo, W. Yang, D. Wang, J. Peng, Y. Cao, Efficient electron injection from a bilayer cathode consisting of aluminum and alcohol-/water-soluble conjugated polymer, Adv. Mater. 16 (2004) 1826–1830.

[17] (a) M.Y. Jo, Y.E. Ha, J.H. Kim, Polyviologen derivatives as an interfacial layer in polymer solar cells, Sol. Energy Mater. Sol. Cells 107 (2012) 1–8;
(b) C. Liu, Y. Tan, C. Li, F. Wu, Y. Chen, Enhanced power-conversion efficiency in inverted bulk heterojunction solar cells using liquid-crystal-conjugated polyelectrolyte interlayer, ACS Appl. Mater. Interfaces 7 (2015) 19024–19044;
(c) L. Chen, C. Xie, Y. Chen, Self-assembled conjugated polyelectrolyte-ionic liquid crystal complex as an interlayer for polymer solar cells: achieving performance enhancement via rapid liquid crystal-induced dipole orientation, Macromolecules 47 (2014) 1623–1632;
(d) L. Huang, L. Chen, P. Huang, F. Wu, L. Tan, S. Xiao, W. Zhong, L. Sun, Y. Chen, Triple dipole effect from self-assembled small-molecules for high performance organic photovoltaics, Adv. Mater. 28 (2016) 4852–4860.

[18] M.Y. Jo, Y.E. Ha, J.H. Kim, Interfacial layer material derived from dialkylviologen and sol–gel chemistry for polymer solar cells, Org. Electron. 14 (2013) 995–1001.

[19] G.E. Lim, Y.E. Ha, M.Y. Jo, J. Park, Y.C. Kang, J.H. Kim, Nonconjugated anionic polyelectrolyte as an interfacial layer for the organic optoelectronic devices, ACS Appl. Mater. Interfaces 5 (2013) 6508–6513.

[20] H. Wang, W. Zhang, C. Xu, X. Bi, B. Chen, S. Yang, Efficiency enhancement of polymer solar cells by applying poly(vinylpyrrolidone) as a cathode buffer layer via spin coating or self-assembly, ACS Appl. Mater. Interfaces 5 (2013) 26–34.

[21] F. Zhang, M. Ceder, O. Inganas, Enhancing the photovoltage of polymer solar cells by using a modified cathode, Adv. Mater. 19 (2007) 1835–1838.

[22] Y.E. Ha, G.E. Lim, M.Y. Jo, J. Park, Y.C. Kang, S.J. Moon, J.H. Kim, Enhancing the efficiency of opto-electronic devices by the cathode modification, J. Mater. Chem. C 2 (2004) 3820–3825.

[23] X. Liu, R. Xu, C. Duan, F. Huang, Y. Cao, Non-conjugated water/alcohol soluble polymers with different oxidation states of sulfide as cathode interlayers for high-performance polymer solar cells, J. Mater. Chem. C 4 (2016) 4288–4295.

[24] W. Xu, Z. Kan, T. Ye, L. Zhao, W.-Y. Lai, R. Xia, G. Lanzani, P.E. Keivanidis, W. Huang, Well-defined star-shaped conjugated macroelectrolytes as efficient electron-collecting interlayer for inverted polymer solar cells, ACS Appl. Mater. Interfaces 7 (2015) 452–459.

[25] Z. Wang, Z. Li, X. Xu, Y. Li, K. Li, Q. Peng, Stimuli-directing self-organized 3D liquid-crystalline nanostructures: from materials design to photonic applications, Adv. Funct. Mater. 26 (2016) 1–10.

[26] T.T. Do, H.S. Hong, Y.E. Ha, G.E. Lim, Y.S. Won, J.H. Kim, Investigation of the effect of conjugated polyelectrolyte as a cathode buffer layer on the photovoltaic properties, Synth. Met. 198 (2014) 122–130.

[27] T.T. Do, H.S. Hong, Y.E. Ha, S.I. Yoo, Y.S. Won, M.J. Moon, J.H. Kim, Synthesis and characterization of conjugated oligoelectrolytes based on fluorene and carbazole derivative and application of polymer solar cell as a cathode buffer layer, Macromol. Res. 23 (2015) 367–376.

[28] C. Min, C. Shi, W. Zhang, T. Jiu, J. Chen, D. Ma, J. Fang, A small-molecule zwitterionic electrolyte without a π-delocalized unit as a charge-injection layer for high-performance PLEDs, Angew. Chem. Int. Ed. 52 (2013) 3417–3420.

[29] Z. Liu, X. Ouyang, R. Peng, Y. Bai, D. Mi, W. Jiang, A. Facchetti, Z. Ge, Efficient polymer solar cells based on the synergy effect of a novel non-conjugated small-molecule electrolyte and polar solvent, J. Mater. Chem. A 4 (2016) 2530–2536.

[30] X. Li, W. Zhang, X. Wang, Y. Wu, F. Gao, J. Fang, Critical role of the external bias in improving the performance of polymer solar cells with a small molecule electrolyte interlayer, J. Mater. Chem. A 3 (2015) 504–508.

[31] J.H. Seo, A. Gutacker, Y.M. Sun, H.B. Wu, F. Huang, Y. Cao, U. Scherf, A.J. Heeger, G.C. Bazan, Improved high-efficiency organic solar cells via incorporation of a conjugated polyelectrolyte interlayer, J. Am. Chem. Soc. 133 (2011) 8416–8419.

[32] S. Nam, J. Jang, H. Cha, J. Hwang, T.K. An, S. Park, C.E. Park, Effects of direct solvent exposure on the nanoscale morphologies and electrical characteristics of PCBM-based transistors and photovoltaics, J. Mater. Chem. 22 (2012) 5543–5549.

[33] H.Q. Zhou, Y. Zhang, J. Seifter, S.D. Collins, C. Luo, G.C. Bazan, T.Q. Nguyen, A.J. Heeger, High-efficiency polymer solar cells enhanced by solvent treatment, Adv. Mater. 25 (2013) 1646–1652.

[34] Z.K. Tan, Y. Vaynzof, D. Credgington, C. Li, M.T.L. Casford, A. Sepe, S. Huettner, M. Nikolka, F. Paulus, L. Yang, H. Sirringhaus, N.C. Greenham, R.H. Friend, In-situ switching from barrier-limited to ohmic anodes for efficient organic optoelectronics, Adv. Funct. Mater. 24 (2014) 3051–3058.

[35] Y. Wang, Y. Liu, S. Chen, R. Peng, Z. Ge, Significant enhancement of polymer solar cell performance via side-chain engineering and simple solvent treatment, Chem. Mater. 25 (2013) 3196–3204.

[36] A. Bagui, S.S.K. Iyer, Increase in hole mobility in poly (3-hexylthiophene-2,5-diyl) films annealed under electric field during the solvent drying step, Org. Electron. 15 (2014) 1387–1395.

[37] V.D. Mihailetchi, J.K. van Duren, P.W. Blom, J.C. Hummelen, R.A. Janssen, J.M. Kroon, M.T. Rispens, W.J.H. Verhees, M.M. Wienk, Electron transport in a methanofullerene, Adv. Funct. Mater. 13 (2003) 43–46.